ELSEVIER

Carbohydrate Polymers 51 (2003) 177–182

Carbohydrate Polymers

www.elsevier.com/locate/carbpol

Surfactant-mediated solubilisation of amylose and visualisation by atomic force microscopy

A. Patrick Gunning[a,*], Thierry P. Giardina[b], Craig B. Faulds[a], Nathalie Juge[b], Steven G. Ring[a], Gary Williamson[a], Victor J. Morris[a]

[a]*Institute of Food Research, Norwich Research Park, Colney, Norwich NR4 7UA, UK*
[b]*Institute Mediterraneen de Recherche en Nutrition, UMR INRA 1111, Faculté des Sciences de St Jérôme, Av. Escadrille Normandie-Niemen, Marseilles F-13397 Cedex 20, France*

Received 26 October 2001; accepted 2 May 2002

Abstract

The starch polysaccharide amylose has been visualised at the molecular level by atomic force microscopy (AFM). In order to image individual amylose chains, a new method was developed for producing aqueous amylose solutions at room temperature. The method involved incubation of hot amylose solutions with iodine and the non-ionic surfactant Tween-20 (polyoxyethylene sorbitan monolaurate). This process stabilises the amylose molecules such that, after cooling to room temperature, no aggregation takes place. AFM images of the resulting sample revealed a distribution of extended chain-like molecules, and allowed for the first time, direct visualisation of a small number of branched macromolecules. Treatment of the sample with the starch-degrading bacterial α-amylase (EC 3.2.1.1) confirmed the nature of the soluble chain-like polymers.

Keywords: Atomic force microscopy; Amylose; Branching; α-Amylase; Tween-20

1. Introduction

Starch is the major plant polysaccharide consumed by mankind and is found in nature as complex semi-crystalline granules (Gallant, Bouchet, & Baldwin, 1997). Two classes of polysaccharide can be extracted from starch: amylopectin and amylose. Amylopectin is a complex branched α-D-glucan and amylose is essentially a linear homopolymer composed of 1,4 linked α-D-glucose. However, detailed chemical analysis has suggested some degree of branching of amylose molecules (Hizukuri, Shirasaka, & Juliano, 1983a; Hizukuri, Takeda, Yasuda, & Suzuki, 1983b; Mua & Jackson, 1998; Takeda, Maruta, & Hizukuri, 1992a,b). A thorough characterisation of these branched structures would involve determining the percentage of branched molecules within the population, and the size and distribution of branches on discrete molecules. Such studies require the visualisation of individual amylose molecules.

Atomic force microscopy (AFM) has been applied successfully to visualise a range of polysaccharides from various sources including land plants (Baker, Helbert, Sugiyama, & Miles, 1997, 1998, 2000; Gunning et al., 2000; Hanley, Gaisson, Revel, & Gray, 1992; McIntire & Brant, 1999; Round, MacDougall, Ring, & Morris, 1997; Round, Rigby, MacDougall, Ring, & Morris, 2001), algae (Gunning et al., 1998; McIntire & Brant, 1997, 1999), animals (Cowman, Li, & Balazs, 1998; Gunning, Morris, Al-Assaf, & Phillips, 1996) and bacteria (Kirby, Gunning, & Morris, 1996; McIntire & Brant, 1998; McIntire, Penner, & Brant, 1995; Vuppu, Garcia, & Vernia, 1997). Factors such as molecular branching (Round et al., 1997, 2001), molecular weight distribution (McIntire & Brant, 1999; Ridout, Brownsey, Gunning, & Morris, 1998), helical pitch (Kirby, Gunning, Morris, & Ridout, 1995), molecular conformation (McIntire & Brant, 1998), interactions involved in supra-molecular assembly (McIntire & Brant, 1997), cell wall structure (Kirby, Gunning, Waldron, Morris, & Ng, 1996), and gelation (Gunning, Kirby, Ridout, Brownsey, & Morris, 1996) have all been investigated by AFM. However there has only been one report on AFM imaging of amylose (McIntire & Brant, 1999). The present study reports a method for solubilising amylose at room temperature that allows direct visualisation of individual amylose chains. This has enabled characterisation of the

* Corresponding author. Tel.: +44-1603-255201; fax: +44-1603-507723.
E-mail address: patrick.gunning@bbsrc.ac.uk (A.P. Gunning).

0144-8617/03/$ - see front matter
PII: S0144-8617(02)00126-1

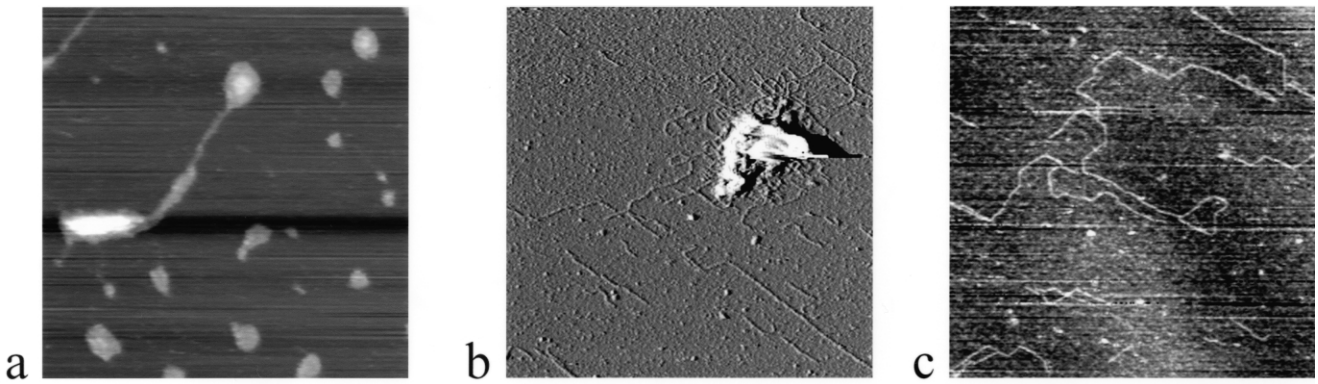

Fig. 1. AFM images of amylose on mica, imaged under butanol. (a) Deposited from hot amylose solutions, scan size: 600 nm × 600 nm, (b) error signal image showing partial dissolution of an amylose aggregate, scan size: 1.2 μm × 1.2 μm, (c) deposited from room temperature amylose solutions containing iodine and the surfactant Tween-20, scan size: 1.6 μm × 1.6 μm.

molecular size and polydispersity of the amylose molecules, and permitted visualisation of molecular branching for the first time.

2. Experimental

2.1. Solubilisation of amylose

Amylose was extracted from pea starch granules by aqueous leaching at 70 °C, followed by precipitation of the amylose as a 1-butanol complex (Ring, I'Anson, & Morris, 1985). The aqueous complex was heated to 90 °C and the butanol driven off by bubbling argon through the hot solution for 30 min. This procedure produced a clear, viscous hot (90 °C) solution of amylose in water, with a concentration of around 30 mg ml^{-1}. When this solution was cooled to room temperature it became unstable and the amylose precipitated from solution. A protocol was therefore developed which overcame this problem and resulted in a stable solution containing discrete, unaggregated amylose chains, even at room temperature. An aliquot of the hot amylose solution was diluted into hot water (90 °C) using a preheated Gilson™ pipette tip (this procedure had to be done quickly in order to minimise cooling of the solution and thus the risk of re-aggregation) to a concentration of approximately 3 mg ml^{-1}. The hot dilute solution was then diluted once more in hot water (90 °C) to a final amylose concentration of approximately 3 μg ml^{-1}. A two-step dilution was carried out in order to allow a reasonable quantity (0.5 ml) of the concentrated amylose solution to be transferred; smaller volumes resulted in rapid cooling of the concentrated solution, which led to an irreversible aggregation of the amylose chains. Iodine solution (0.05 M aqueous stock, Fisher Scientific, UK) was added to the hot 3 μg ml^{-1} amylose solution to produce a final concentration of 5 μM I_2, in order to promote helix formation of the amylose molecules on cooling. Cooling these samples to room temperature still led to aggregation of the amylose molecules. For the pea amylose samples addition of Tween-20, to a concentration of 1.6 mM, prevented re-aggregation of the amylose chains upon cooling. After the addition of Tween-20 the amylose solution was held at 90 °C for 12 h before being allowed to cool to room temperature. Tween-20 (molecular weight 1230) was purchased as a 10% solution (Surfact-Amps 20) from Pierce (Rockford, USA).

2.2. Enzymatic degradation

α-Amylase from *Bacillus licheniformis* [EC 3.2.1.1, Heat stable, 95% purity SDS-PAGE] was purchased from Sigma Chemicals, UK. Partial hydrolysis of amylose was carried out by incubation of 1 ml of the 3 μg ml^{-1} amylose/Tween-20/iodine stock solution with 20 μl of 10 μg ml^{-1} α-amylase solution for various periods of time. Hydrolysis was stopped by the addition of propan-2-ol to the reaction mixture to a final alcohol concentration of 17% w/v.

2.3. Atomic force microscopy and image analysis

Amylose solutions or dispersions were drop deposited (2 μl) onto freshly cleaved mica, and then imaged under redistilled *n*-butanol. The AFM was manufactured by ECS Ltd (Cambridge, UK). The probes used were Nanoprobe™ (Digital Instruments, Santa Barbara CA, USA) oxide-sharpened cantilevers with a quoted force constant of 0.38 N m^{-1}. The microscope was operated in the constant force mode (dc-mode). The imaging force was maintained in the range 1–3 nN. Molecular lengths were quantified using ImagePro (Media Cybernetics, USA) by manually tracing the contours of the molecules in the AFM images. Overlapping molecules and any that appeared to go over the edges of an image area were excluded from the measurements.

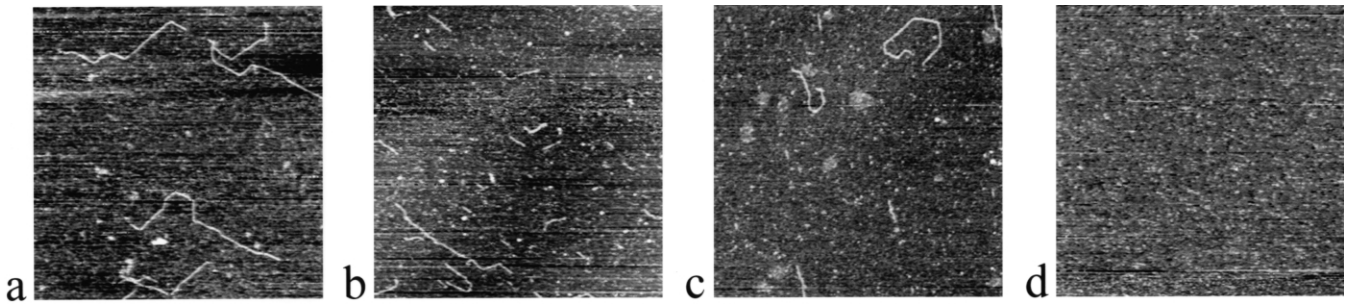

Fig. 2. Sequence of AFM images of the degradation of iodine-Tween-20 solubilised amylose molecules by α-amylase, obtained by sampling after various time points (a) 0 min, no added enzyme, (b) 10 min, (c) 30 min, (d) 60 min. All scan sizes: 1.2 μm × 1.2 μm.

3. Results and discussion

When the amylose butanol complex is simply dispersed in water at high temperature, the butanol removed, and the sample cooled to room temperature, then the amylose precipitates, even from dilute solutions. Fig. 1a shows AFM images of apparent small amylose aggregates precipitated from solution and drop deposited onto mica. These aggregates prevent visualisation of individual molecules. In the present study we show that addition of iodine and the non-ionic surfactant Tween-20 to the hot amylose solution can prevent aggregation on cooling to room temperature. Fig. 1b shows an AFM image of a cooled partially aggregated sample. The AFM image clearly shows chains, believed to be amylose molecules, emanating from the aggregate, and also discrete chains lying alongside the aggregate. However, even if the chains are amylose molecules then most of the chains are still 'locked up' in aggregates, and those chains that are visible are unrepresentative of the native population of amylose molecules. Fig. 1c shows that by varying the amounts of iodine and Tween-20 it is possible to reach a situation whereupon aggregation of the amylose on cooling is completely prevented. Fig. 1c demonstrates that under these optimal conditions only discrete and extended polymer molecules can be seen in the AFM images.

In order to confirm the nature of the observed molecules we used α-amylase, an enzyme involved in amylose degradation. Fig. 2a–d shows a series of representative

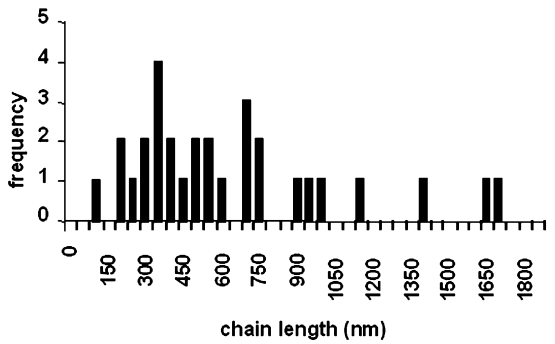

Fig. 3. Data obtained from the analysis of AFM images, quantifying the variation in the distribution of amylose chain lengths.

AFM images obtained after the treatment of the amylose–iodine–Tween-20 complex solutions with α-amylase. The images were obtained at four time intervals, defined according to the time at which the enzyme was rendered inactive by the addition of propan-2-ol. Aliquots of these partially digested samples were then deposited onto mica and imaged using the AFM. The first image in the set (Fig. 2a) was obtained before the addition of the enzyme, and is defined as the zero time point. The image reflects the distribution of chain lengths for the 'native' un-degraded amylose. After incubation of the amylose complex solution with the enzyme for 10 min many more short chains are visible in the AFM images (Fig. 2b). The image also reveals that, in addition to the short chains, a few longer chains of comparable length to those seen in the untreated sample are still present. The AFM image in Fig. 2c was obtained after incubation with the enzyme for 30 min, and reveals that most of the short chains have been degraded, but that there are still some longer chains present. The final AFM image (Fig. 2d) in the sequence shows that at sufficiently long times (60 min) no chains could be found, despite extensive searching of the surface. This confirms the nature of the extended chains visualised after treatment of the hot amylose solutions with iodine-Tween-20, and shown in Fig. 1b,c, since α-amylase attacks only α-1,4-linked glucans. The images also demonstrate that AFM can be used to follow events that alter chain length, such as enzymatic hydrolysis, of individual molecules, and could be used to test quantitatively different models of enzymic degradation.

No preferential orientation of the molecules was observed and thus the extended appearance suggests that the amylose is a stiff, probably helical structure: AFM images of flexible random coil state polysaccharides appear as globular structures, representing a time-averaged conformation of the molecules (Tasker et al., 1996). It has been demonstrated previously that amylose can form complexes with fatty acids. Molecular modelling of such complexes has shown that the aliphatic chains of the fatty acids sit inside the amylose helices, whilst the polar head groups of the fatty acids are excluded (Godet, Buleon, Tran, & Colonna, 1993; Godet, Tran, Colonna, Buleon, & Pezolet, 1995). Furthermore, the affinity of cyclic forms of amylose

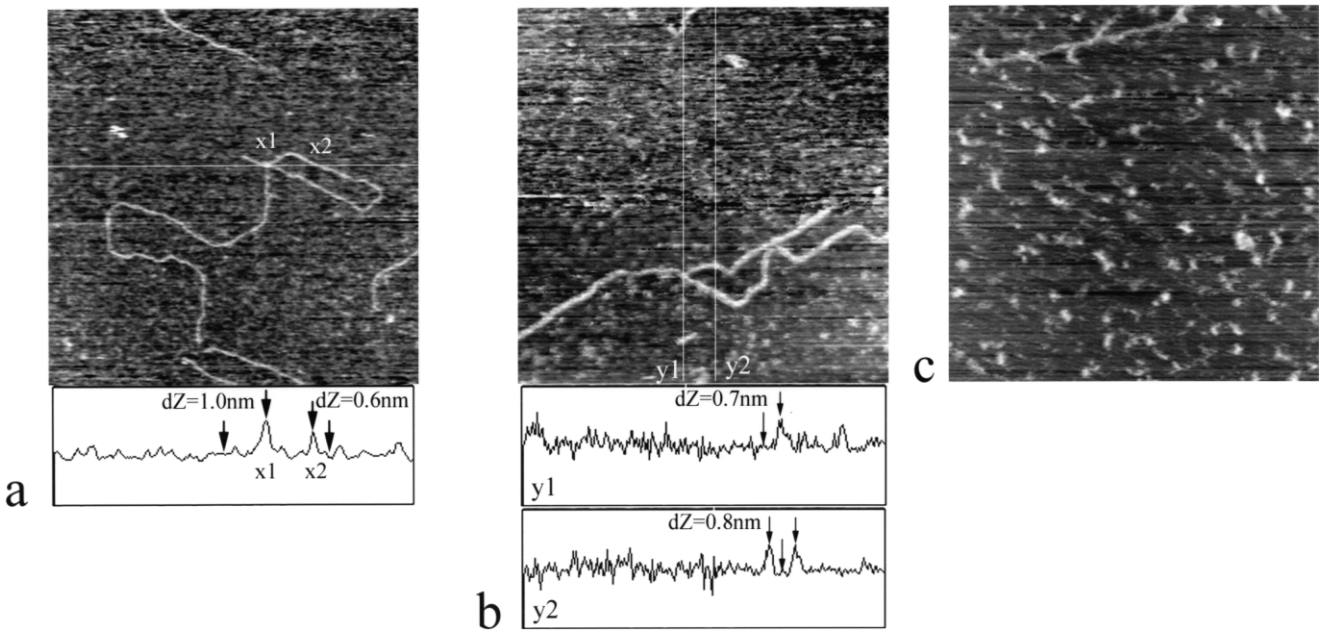

Fig. 4. AFM images of amylose/iodine/Tween-20 preparations that have been deposited onto mica. (a) Overlapping amylose molecules, scan size: 800 nm × 800 nm. (b) Branched amylose molecule showing a single long branch, scan size: 600 nm × 600 nm. Line profiles beneath the images are taken along the white lines marked on each scan. (c) Branched amylose molecule displaying short branches, scan size: 800 nm × 800 nm.

for detergents such as the Tweens, which are composed of aliphatic chains terminated with polar head groups, has also been demonstrated recently (Machida et al., 2000). We can thus postulate that the extended structures seen in Fig. 1c, and produced by solubilisation of amylose with iodine and Tween-20 are due to complex formation. In this hypothesis the iodine and the lauryl chain of the Tween-20 molecule would be incorporated into the amylose helix and the polar head-group of the Tween (a sorbitan ring linked to a number of oxyethylene moities) would be left protruding, increasing the solubility of the amylose, thus preventing aggregation of the helices upon cooling. This non-destructive method of solubilisation allows the visualisation of single amylose molecules.

Because the amylose molecules appear as discrete and extended entities in the AFM images it is possible to determine the distribution of chain lengths and the polydispersity of the sample. From the histogram of chain lengths shown in Fig. 3 it is possible to calculate the weight (L_W) and number (L_N) average chain lengths and, from the ratio $L_W/L_N = 1.4$, the polydispersity index. The expected rise per monomer unit is 0.135 nm for a V-type single helix. Based on this value, the calculated weight average 'molecular weight' is 1.08×10^6, which is in reasonably good agreement with the value of 0.84×10^6, obtained from previous light scattering data on pea amylose samples, isolated by the same procedure and involving leaching between 70–75 °C (Ring et al., 1985). The measured heights of the chains are 0.6–0.7 nm, similar to the value of 0.54 nm found for synthetic amylose (McIntire & Brant, 1999). McIntire and Brant (1999) concluded that their synthetic amylose samples adopted a single helical structure in aqueous solution.

The AFM images of the type shown in Fig. 4 show that a small number of the amylose chains appear to be branched, consistent with previous deductions from chemical analysis data (Hizukuri et al., 1983a,b; Mua & Jackson, 1998; Takeda et al., 1992a,b). Branching can be distinguished from entanglement and crossover points on the molecules through height measurements. Regions where chains cross each other produce a doubling of height, which can be seen as a bright spot in the AFM image in Fig. 4a, and is quantified in the line profile beneath the image. Branch points by contrast exhibit no significant change of height compared to the rest of the chain (Fig. 4b). Only a very few branched molecules were observed. Fig. 4b and c illustrates two different types of branching patterns that were observed: a linear backbone containing a single long branch (Fig. 4b) and a linear backbone containing several short branches (Fig. 4c). These studies demonstrate that AFM can be used to characterise branching of amylose molecules. Such studies could assist in understanding the effects of genetic modifications on the structure and functional properties of starch. A range of isogenic mutants has been developed in peas that are known to affect defined steps in the starch biosynthetic pathway (Denyer et al., 1995; Harrison, Hedley, & Wang, 1998; Hedley, Bogracheva, Lloyd, & Wang, 1996; Hylton & Smith, 1992; Wang et al., 1994; Wang, Bogracheva, & Hedley, 1998). All these mutants produce starches that differ in composition and functional properties (Bogracheva et al., 1999). The *r* and *rug 5* mutations result in significant decreases in the amount

of amylopectin within the starch, without an equivalent decrease in the level of crystallinity of the granules (Bogracheva et al., 1999), suggesting that material normally regarded as amylose is contributing to the crystalline regions within the granules. AFM experiments of the type described here could be used to help determine whether this contribution involves normal linear amylose molecules, or is a consequence of the presence of larger quantities of 'intermediate' branched amylose molecules.

4. Conclusions

A new method allowing the production of stable unaggregated aqueous solutions of pea starch amylose at room temperature has been developed. AFM images were obtained for samples prepared by drop deposition of the solutions onto mica. Degradation of the samples with α-amylase was used to confirm the nature of the observed molecules. The images suggest that the amylose adopts a 'V-helical' structure, which could be due to formation of an inclusion complex with iodine and the lipid sidechains of the Tween-20 molecules. The chain length distribution of the amylose molecules was measured directly from the AFM images, allowing characterisation of the molecular size, mass and polydispersity. AFM imaging has also allowed direct visualisation, for the first time, of molecular branching of amylose molecules and two distinct types of branched structure have been observed.

Acknowledgments

Dr Louise Botham is thanked for preparation of the amylose–butanol complex used in this study. We are grateful to the Biotechnology and Biological Sciences Research Council, UK, and the European Commission Framework 4 BIOTECH 2 Programme (BIO4980022), for generous financial support.

References

Baker, A. A., Helbert, W., Sugiyama, J., & Miles, M. J. (1997). High-resolution atomic force microscopy of native Valonia cellulose I microcrystals. *Journal of Structural Biology*, *119*, 129–138.

Baker, A. A., Helbert, W., Sugiyama, J., & Miles, M. J. (1998). Surface structure of native cellulose microcrystals by AFM. *Applied Physics A*, *66*, S559–S563.

Baker, A. A., Helbert, W., Sugiyama, J., & Miles, M. J. (2000). New insights into cellulose structure by atomic force microscopy shows the I-alpha crystal phase at near-atomic resolution. *Biophysical Journal*, *79*, 1139–1145.

Bogracheva, T. Ya., Cairns, P., Noel, T. R., Hulleman, S., Wang, T. L., Morris, V. J., Ring, S. G., & Hedley, C. L. (1999). The effect of mutant genes at the *r*, *rb*, *rug 3*, *rug 4*, *rug 5* and *lam* loci on the granular structure and physico-chemical properties of pea seed starch. *Carbohydrate Polymers*, *39*, 303–314.

Cowman, M. K., Li, M., & Balazs, E. A. (1998). Tapping mode AFM of hyaluronan polysaccharide on mica in air: Extended and intramolecularly interacting chains. *Biophysical Journal*, *75*, 2030–2037.

Denyer, K., Barber, L. R., Burton, R., Hedley, C. L., Hylton, C. M., Johnson, S., Jones, D. A., Marshall, J., Smith, A. M., Tatge, H., Tomlinson, K., & Wang, T. L. (1995). The isolation and characterisation of novel low-amylose mutants of *Pisum sativum* L. *Plant Cell and Environment*, *18*, 1019–1026.

Gallant, D. J., Bouchet, B., & Baldwin, P. M. (1997). Microscopy of starch: Evidence of a new level of granule organization. *Carbohydrate Polymers*, *32*, 177–191.

Godet, M. C., Buleon, A., Tran, V., & Colonna, P. (1993). Structural features of fatty acid–amylose complexes. *Carbohydrate Polymers*, *21*, 91–95.

Godet, M. C., Tran, V., Colonna, P., Buleon, A., & Pezolet, M. (1995). Inclusion exclusion of fatty acids in amylose complexes as a function of the fatty acid chain length. *International Journal of Biological Macromolecules*, *17*, 405–408.

Gunning, A. P., Cairns, P., Round, A. N., Bixler, H. J., Kirby, A. R., & Morris, V. J. (1998). Characterising semi-refined iota carrageenan networks by atomic force microscopy. *Carbohydrate Polymers*, *36*, 67–72.

Gunning, A. P., Kirby, A. R., Ridout, M. J., Brownsey, G. J., & Morris, V. J. (1996). Investigation of gellan networks and gels by atomic force microscopy. *Macromolecules*, *29*, 6791–6796.

Gunning, A. P., Mackie, A. R., Kirby, A. R., Kroon, P., Williamson, G., & Morris, V. J. (2000). Motion of a cell wall polysaccharide observed by atomic force microscopy. *Macromolecules*, *33*, 5680–5685.

Gunning, A. P., Morris, V. J., Al-Assaf, S., & Phillips, G. O. (1996). Atomic force microscopic studies of hylan and hyaluronan. *Carbohydrate Polymers*, *30*, 1–8.

Hanley, S. J., Gaisson, J., Revel, J.-F., & Gray, D. (1992). Atomic force microscopy of cellulose microfibrils—Comparison with transmission electron microscopy. *Polymer*, *33*, 4639–4642.

Harrison, C. J., Hedley, C. L., & Wang, T. L. (1998). Evidence that the rug 3 locus of pea *Pisum sativum* L. encodes plastidial phosphoglucomutase confirms that the imported substrate for starch synthesis in pea is glucose-6-phosphate. *The Plant Journal*, *13*, 753–762.

Hedley, C. L., Bogracheva, T. Ya., Lloyd, J. R., & Wang, T. L. (1996). Manipulation of starch composition and quality in peas. In G. R. Fenwick, C. L. Hedley, R. L. Richardson, & S. Khokhar (Eds.), *Agri-food 95. An interdisciplinary approach* (p. 138) Cambridge: Royal Society of Chemistry.

Hizukuri, S., Shirasaka, K., & Juliano, B. (1983a). Phosphorous and amylose branching in rice starch granules. *Starch*, *35*, 348–350.

Hizukuri, S., Takeda, Y., Yasuda, M., & Suzuki, A. (1983b). Multi-branched nature of amylose and the action of de-branching enzymes. *Carbohydrate Research*, *94*, 205–213.

Hylton, C., & Smith, A. M. (1992). The *rb* mutation of peas causes structural and regulatory changes in ADP glucose pyrophosphorylase from developing embryos. *Plant Physiology*, *99*, 1626–1634.

Kirby, A. R., Gunning, A. P., & Morris, V. J. (1996). Imaging polysaccharides by atomic force microscopy. *Biopolymers*, *38*, 355–366.

Kirby, A. R., Gunning, A. P., Morris, V. J., & Ridout, M. J. (1995). Observation of the helical structure of the bacterial polysaccharide acetan by atomic force microscopy. *Biophysical Journal*, *68*, 360–363.

Kirby, A. R., Gunning, A. P., Waldron, K. W., Morris, V. J., & Ng, A. (1996). Visualisation of plant cell walls by atomic force microscopy. *Biophysical Journal*, *70*, 1138–1143.

Machida, S., Ogawa, S., Xiaohua, S., Takaha, T., Fujii, K., & Hayashi, K. (2000). Cycloamylose as an efficient artificial chaperone for protein refolding. *FEBS Letters*, *486*, 131–135.

McIntire, T. M., & Brant, D. A. (1997). Imaging of individual biopolymers and supramolecular assemblies using non-contact atomic force microscopy. *Biopolymers*, *42*, 133–146.

McIntire, T. M., & Brant, D. A. (1998). Observation of the (1 → 3) beta-D-

glucan linear triple helix to macrocycle interconversion using non-contact atomic force microscopy. *Journal of the American Chemical Society*, *120*, 6909–6919.

McIntire, T. M., & Brant, D. A. (1999). Imaging of carrageenan macrocycles and amylose by non-contact atomic force microscopy. *International Journal of Biological Macromolecules*, *26*, 310–313.

McIntire, T. M., Penner, R. M., & Brant, D. A. (1995). Observations of a circular, triple helical polysaccharide using non-contact atomic force microscopy. *Macromolecules*, *28*, 6375–6377.

Mua, J. P., & Jackson, D. S. (1998). Retrogradation and gel textural attributes of corn starch amylose and amylopectin fractions. *Journal of Cereal Science*, *27*, 157–166.

Ridout, M. J., Brownsey, G. J., Gunning, A. P., & Morris, V. J. (1998). Characterisation of the polysaccharide produced by *Acetobacter xylinum* strain CR1/4 by light scattering and atomic force microscopy. *International Journal of Biological Macromolecules*, *23*, 287–293.

Ring, S. G., I'Anson, K., & Morris, V. J. (1985). Static and dynamic light scattering studies of amylose solutions. *Macromolecules*, *18*, 182–188.

Round, A. N., MacDougall, A. J., Ring, S. G., & Morris, V. J. (1997). Unexpected branching in pectins observed by atomic force microscopy. *Carbohydrate Research*, *303*, 251–253.

Round, A. N., Rigby, N. M., MacDougall, A. J., Ring, S. G., & Morris, V. J. (2001). Investigating the nature of branching in pectin by atomic force microscopy and carbohydrate analysis. *Carbohydrate Research*, *331*, 337–342.

Takeda, Y., Maruta, N., & Hizukuri, S. (1992a). Examination of the structure of amylose by titration labelling of the reducing terminal. *Carbohydrate Research*, *227*, 113–120.

Takeda, Y., Maruta, N., & Hizukuri, S. (1992b). Structure of amylose subfractions with different molecular sizes. *Carbohydrate Research*, *226*, 279–285.

Tasker, S., Matthijs, G., Davies, M. C., Roberts, C. J., Schacht, E. H., & Tendler, S. J. B. (1996). Molecular resolution imaging dextran monlayers immobilised on silica by atomic force microscopy. *Langmuir*, *12*, 6436–6442.

Vuppu, A. K., Garcia, A. A., & Vernia, C. (1997). Tapping mode atomic force microscopy of scleroglucan network. *Biopolymers*, *42*, 89–100.

Wang, T. L., Barber, R. A., Denyer, K., Hedley, C. L., Hylton, C. M., Johnson, S., Jones, D. A., Marshall, J., Smith, A. M., Tatge, H., & Tomlinson, K. L. (1994). Seed mutants in *Pisum*: *lam* (low amylose) a new loci affecting starch composition. *Pisum Genetics*, *26*, 39–40.

Wang, T. L., Bogracheva, T. Ya., & Hedley, C. L. (1998). Starch: As simple as A, B, C? *Journal of Experimental Botany*, *49*, 481–502.